

PIPE FLOW TURBULENCE AT EXTREME REYNOLDS NUMBERS

Alexander J. Smits, Marcus Hultmark, Margit Vallikivi, Brian J. Rosenberg

Department of Mechanical and Aerospace Engineering
Princeton University
Princeton, NJ 08544, USA
asmits@princeton.edu

and Sean C. C. Bailey

Department of Mechanical Engineering
University of Kentucky
Lexington, KY 40506, USA

ABSTRACT

Turbulent fluid motion is characterized by a large range of physical and temporal scales, so that the smallest eddies are typically many orders of magnitude smaller than the largest eddies, and the time scales also encompass many orders of magnitude. This complexity makes turbulent flows extremely difficult to predict and so experiments become crucial in any effort to model the flow behavior. It is the same complexity, however, that makes turbulence measurements very difficult, and current methods often suffer from inadequate spatial and temporal resolution to capture the full range of scales present in the flow. We describe a new nano-scale anemometry probe that dramatically extends the range of possible turbulence measurements, and we demonstrate its impact by presenting turbulence measurements in a pipe flow over an unprecedented range of conditions. The results reveal a remarkable similarity in the scaling for the mean flow and for the streamwise turbulence intensity, which marks the onset of what we call the extreme Reynolds number regime.

INTRODUCTION

The behavior of wall-bounded turbulence at very high Reynolds numbers is of great interest due to the many practical applications that encounter high Reynolds number turbulence, and because most turbulence theory is based on the concept of sufficient separation of scales where the energy-containing motions are distinct from the dissipating motions, which only occurs at high Reynolds number. In that respect, the relevant Reynolds number can be defined as the ratio of the largest scales of motion to the smallest ones, which for pipe flow would be $R^+ = Ru_\tau/\nu$, where R is the pipe radius, u_τ is the friction velocity ($= \sqrt{\tau_w/\rho}$), τ_w is the wall shear stress, and ρ and ν are the fluid density and kinematic viscosity, respectively.

Here, we are interested in exploring the behavior of turbulence in pipe flow over a large Reynolds number range, specifically $1.1 \times 10^3 \leq R^+ \leq 1.01 \times 10^5$, in order to eluci-

date scaling trends in the turbulence statistics and draw comparisons with the scaling of the mean flow.

The mean flow scaling in high Reynolds number pipe flow, following McKeon et al. [2004], can be divided into four distinct regions. The first is the near-wall region, extending from the wall out to approximately $y^+ = 50$, where the relevant scaling parameters are u_τ and the viscous length scale, ν/u_τ . The near wall region encompasses the viscous-dominated region ($y^+ \leq 5$) and the buffer layer. Here, y is the wall-normal distance, and all “plus” variables are non-dimensionalized using u_τ and ν . Further from the wall, between approximately $y^+ = 50$ and 600, exists a power law region, where the mean velocity follows $U^+ = 8.70(y^+)^{0.137}$. If the Reynolds number is high enough so that a range exists such that $600 \leq y^+ \leq 0.12y/R$, there is a third region where the mean velocity follows a logarithmic law of $U^+ = (1/\kappa)\ln y^+ + B$ and κ and B are constants. Finally, beyond $y/R \approx 0.12$ a fourth region can be observed, referred to as the wake region, where the mean velocity scales with outer variables, that is, it is a function of y/R .

The scaling of the turbulence statistics is less clear. In the viscous region, we know from asymptotic analysis that the non-dimensional streamwise component of the fluctuations $u^{+2} = \overline{u^2}/u_\tau^2$ will vary as $u^{+2} \approx 0.35y^+$. In the buffer layer, near $y^+ = 15$, u^{+2} reaches a maximum and although measurements in boundary layers indicate that this peak increases with Reynolds number, Hultmark et al. [2010] found that in pipe flow the peak remained at a constant level, at least for Reynolds numbers up to $R^+ = 3300$. The streamwise turbulence intensity level then decreases until about $y^+ = 80$, but further from the wall, Morrison et al. [2004] reported on the basis of hot-wire measurements that its behavior depends on Reynolds number, where for $R^+ \geq 10,000$ it begins to increase again to reach a second, outer peak located at a position approximately given by $y^+ = 1.8(R^+)^{0.52}$.

The presence of an outer peak has been disputed, mainly on the grounds that it could be artificially introduced through a form of experimental error experienced in hot-wire anemome-

try referred to as spatial filtering. As the Reynolds number increases for a fixed hot-wire length l , the size of the wire length relative to the smallest turbulent motions increases, causing contributions to the measured turbulence energy from motions smaller than the wire length to become attenuated. Although the precise limit is not known, it seems likely that the non-dimensional wire length l^+ needs to be less than about 5 for the effects of spatial resolution in the near-wall region, where the smallest turbulence scales exist, to be negligible [Smits et al., 2011]. The effect of spatial filtering in the outer region has been studied less extensively, but at the highest Reynolds numbers studied by Morrison et al. $l^+ = 385$, so that spatial filtering undoubtedly had a significant impact, potentially even far from the wall. Given this possibility, the appearance of an outer layer peak in u^{+2} could simply be an artifact of increasing spatial filtering effects as the wall is approached.

The behavior of the streamwise turbulence spectrum, ϕ_{uu} , is yet another question. In the logarithmic region, we expect the low wavenumber region to scale with R , the intermediate wavenumber region to scale with y , and the high wavenumber region to scale with the Kolmogorov length, η . Overlap arguments predict $\phi_{uu} \propto k_x^{-1}$, between the R - and y - scaled regions, and $\phi_{uu} \propto k_x^{-5/3}$, between the y - and η - scaled regions, where k_x is the streamwise wavenumber. Perry et al. [1986], upon integrating this model spectrum, predicted a logarithmic variation in streamwise turbulence intensity, with an additional viscous term that diminishes with increasing Reynolds number. This analysis extended the earlier work by Townsend [1976], who used the attached eddy hypothesis to first suggest a logarithmic variation in the streamwise fluctuations.

To study the behavior of the turbulence fluctuations and the energy spectrum at extreme Reynolds numbers, it is clear that improved turbulence instrumentation is necessary. In particular, much smaller probes are required to reduce the effects of spatial filtering. Here, we use a new class of thermal anemometry probes which are an order of magnitude smaller than conventional hot wires, and we report turbulence measurements in pipe flow over an unprecedented Reynolds number range to demonstrate that the inner peak is invariant with Reynolds number, that the outer peak is a genuine feature of high Reynolds number pipe flow and that its magnitude increases with Reynolds number. Finally, we demonstrate a remarkable symmetry between the scaling of U^+ and u^{+2} , and we report, for the first time, experimental evidence for the logarithmic scaling of the streamwise turbulence over more than one decade in y/R .

EXPERIMENTAL TECHNIQUES

All experiments were conducted in the Princeton Superpipe, as described by Zagarola and Smits [1998] and McKeon et al. [2004]. The facility uses compressed air as the working fluid to obtain Reynolds numbers within the range $35 \times 10^3 \leq Re_D = D\bar{U}/\nu \leq 38 \times 10^6$. The pipe itself was commercial steel, as described by Langelandsvik et al. [2007], with a diameter of 130 mm and an rms roughness height $k_{rms} = 5\mu\text{m}$, with an equivalent sandgrain roughness of $k_s = 1.6k_{rms}$. The flow conditions for each Reynolds number are given in Table 1. It should be noted that for Re_D greater

| Re_D | R^+ | $p(\text{atm})$ | $U_{\text{bulk}}[\text{m/s}]$ | l^+ | $y_0(\mu\text{m})$ |
|-----------|---------|-----------------|-------------------------------|-------|--------------------|
| 42,690 | 1,133 | 0 | 5.0 | 1.0 | 27 |
| 77,920 | 1,922 | 0 | 9.2 | 1.8 | 28 |
| 143,170 | 3,312 | 0 | 16.9 | 3.1 | 28 |
| 243,820 | 5,285 | 0.68 | 17.0 | 4.9 | 28 |
| 471,470 | 9,570 | 2.43 | 16.2 | 8.8 | 28 |
| 721,960 | 14,165 | 3.95 | 17.2 | 13.1 | 28 |
| 1,005,700 | 19,421 | 6.88 | 15.0 | 17.9 | 28 |
| 1,991,900 | 36,876 | 13.3 | 16.5 | 34.1 | 28 |
| 3,867,000 | 69,492 | 22.7 | 19.5 | 64.2 | 28 |
| 5,697,200 | 101,080 | 34.3 | 19.6 | 93.4 | 28 |

Figure 1. Measurement conditions.

than about 7×10^5 the surface roughness begins to have an effect on the friction factor, although Townsend's hypothesis is expected to hold at all Reynolds numbers studied here since $k_{rms}/D = 1/26000$ [see Jiménez, 2004].

To measure the streamwise component of the velocity fluctuations, we used the Nano-Scale Thermal Anemometry Probe (NSTAP) described by Vallikivi et al. [2010] and shown in figure 2. The sensitive element is a $60 \mu\text{m}$ long platinum ribbon, measuring $2 \mu\text{m}$ by 100 nm in cross-section. The frequency response is typically 150 kHz or higher at zero velocity when operated in the constant temperature mode using a Dantec Streamline system, increasing to about 300 kHz at the highest Reynolds number. The data was filtered at 150 kHz using an analog 8 pole Butterworth filter and sampled at 300kHz for all cases. The values of the non-dimensional length l^+ and the distance from the wall to the first measurement point, y_0 , are listed in table 1, where another advantage of using the NSTAP over conventional hot-wires is evident. Namely, the distance from the wall to the first measurement point in the current study was maintained at $28 \mu\text{m}$, which was much closer than was possible using conventional probes, for which some part of the probe would inevitably contact the wall when $y_0 < 80 \mu\text{m}$. Minimizing y_0 is a very important consideration at high Reynolds number in the Superpipe, where the viscous length scale shrinks to smaller than a micron.

RESULTS

First, the performance of the NSTAP was compared to that of a conventional hot-wire in a regime where both probes are expected to have no, or at least little, spatial filtering. The three lowest Reynolds number cases in this study ($Re_D = 45 \times 10^3$, $Re_D = 80 \times 10^3$, and $Re_D = 150 \times 10^3$) match the Reynolds numbers explored by Hultmark et al. [2010], where he used a hot-wire with $2.5 \mu\text{m}$ diameter. The measured streamwise Reynolds stress profiles from both studies are compared in figure 3a, where it is clear that the two probes agree very well in the outer region. In the near-wall region, however, small differences are observed. The NSTAP captures slightly more of the turbulent energy than the hot-wire, especially for the two higher Reynolds numbers. Although l^+ for the hot-wire was within the conventionally accepted length of $l^+ \lesssim 20$, it is clear that the spatial filtering

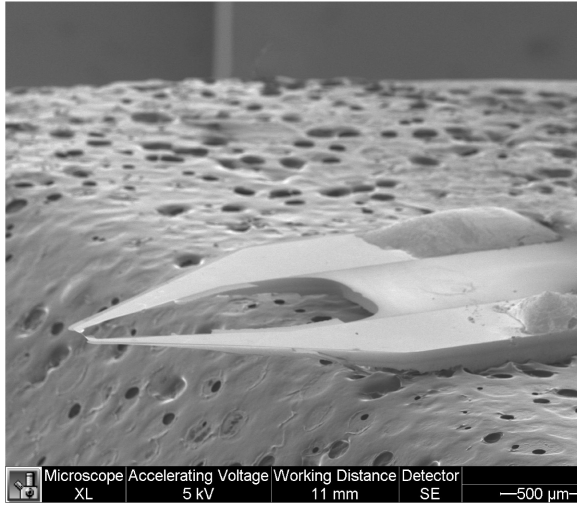


Figure 2. Scanning electron microscope image of a typical NSTAP.

was significant enough to produce a measurable difference between the two probes. This is demonstrated in figure 3b, which shows the same data after applying the correction for spatial filtering effects proposed by Smits et al. [2011]. Once corrected, the results from both probes agree extremely well throughout the depth of the wall layer. As well as highlighting the importance of spatial filtering for even relatively short wire lengths, these results help to demonstrate that the NSTAP performs well as a velocity sensor and that it can provide reliable turbulence measurements.

Figure 4 shows the uncorrected turbulence fluctuations in inner coordinates at $45 \times 10^3 \leq Re_D \leq 5.7 \times 10^6$. In the near-wall region, there is no evidence of an increase in the magnitude of the inner peak with Reynolds number, as has been observed in boundary layers. However, for the four highest Reynolds numbers, a decrease of the magnitude can be seen. This decrease can be attributed to spatial filtering since, although the NSTAP is very small, at the highest Reynolds number $l^+ = 93$. To verify this observation, figure 5 shows the same data corrected for spatial filtering. Here a collapse in the near-wall region can be observed for all Reynolds numbers, confirming the Reynolds number invariance of inner peak magnitude observed by Hultmark et al. [2010], at least up to a Reynolds number $Re_D = 2 \times 10^6$ ($R^+ = 37 \times 10^3$ and $l^+ = 34$, which is the highest Reynolds number where the inner peak is resolved).

Another very interesting feature in the high Reynolds number cases is the existence of an outer peak for $Re_D > 5 \times 10^5$, similar to, and over the same Reynolds number range as, the peak that was observed in the conventional hot-wire measurements by Morrison et al. [2004]. The current results support that the outer peak is a genuine feature of the flow and not an artifact of spatial filtering as previously suggested. As will be clear below, the outer peak is an important feature of high Reynolds number turbulence.

Figure 6 shows the streamwise turbulent fluctuations plotted in outer coordinates for $y^+ > 100$. For high Reynolds number ($Re_D \geq 1 \times 10^6$) the streamwise Reynolds stress has a distinct logarithmic behavior for $y/R < 0.1$. Although

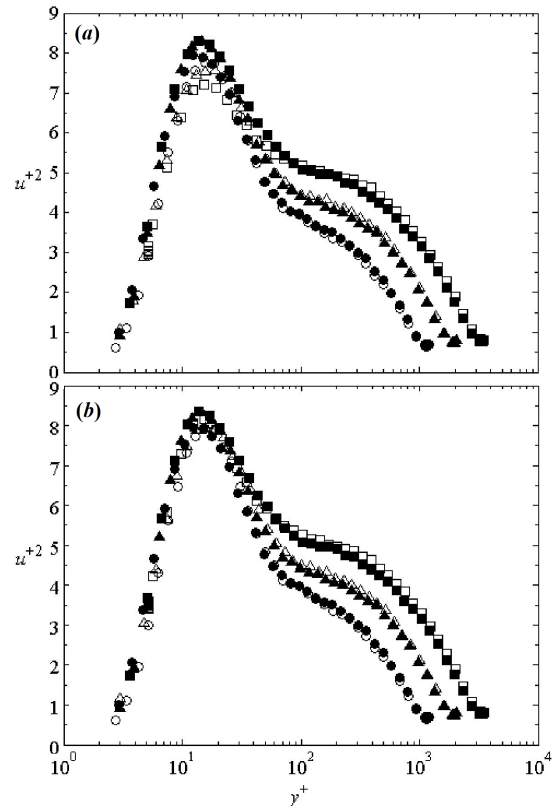


Figure 3. Turbulence intensities at: \circ , $Re_D = 45 \times 10^3$; \triangle , 80×10^3 ; \square , 150×10^3 . Hollow symbols are hot-wire data, and filled symbols are NSTAP data. (a) Uncorrected results and (b) results corrected for spatial filtering using the method of Smits et al. [2011].

Townsend [1976] and Perry et al. [1986] predicted a logarithmic behavior in the turbulence fluctuations for large enough Reynolds numbers, the measurements presented here are the first to show its true evolution, and at the highest Reynolds number it spans more than a decade in y/R . The authors propose that *extreme Reynolds numbers* are those Reynolds numbers where a region exists for which the fluctuations demonstrate a logarithmic behavior. The present results suggest that this occurs when there is a separation between the outer-scaled range, $y/R > 0.1$, and the inner-scaled range, $y^+ < 1000$, which occurs when $Re_\tau > 10^4$. This range is the approximately the same range as that identified by McKeon et al. [2004] for which the mean velocity exhibits truly logarithmic behavior.

At Reynolds numbers where the logarithmically-scaled fluctuations occur, the logarithmic region extends all the way to the outer peak. This suggests that the outer peak forms as a result of increased scale separation between the inner scaled turbulent motions and the outer-scaled turbulent motions. It is interesting to note that the Reynolds number at which the logarithmic behavior becomes evident is roughly the same as when the outer peak emerges.

By comparing profiles of the fluctuating and mean velocities, as is done in figure 7, one can see that the same regions that were defined by McKeon et al. [2004] for the mean ve-

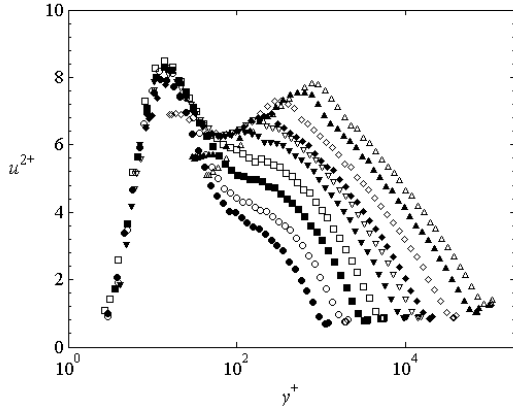


Figure 4. Turbulence intensities in inner variables at $45 \times 10^3 \leq Re_D \leq 5.7 \times 10^6$. All measurements were taken using NSTAP. Uncorrected results.

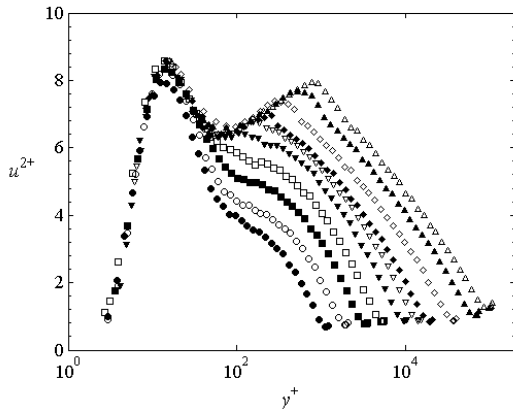


Figure 5. Turbulence intensities in inner variables at $45 \times 10^3 \leq Re_D \leq 5.7 \times 10^6$. All measurements were taken using NSTAP. Results corrected for spatial filtering using the method of Smits et al. 2011.

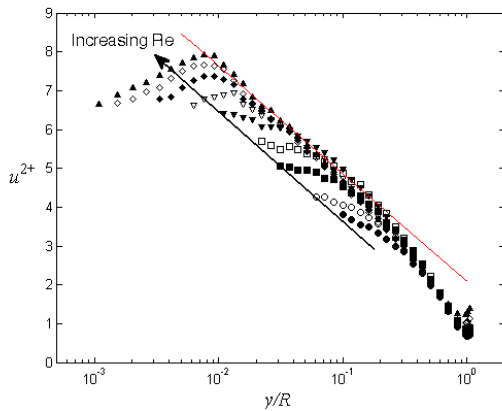


Figure 6. Turbulence intensities in outer variables for $y^+ \geq 100$ at $45 \times 10^3 \leq Re_D \leq 5.7 \times 10^6$. All measurements were taken using NSTAP. Results corrected for spatial filtering using the method of Smits et al. 2011.

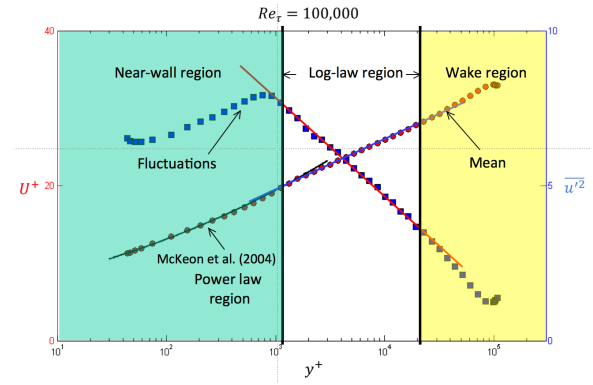


Figure 7. Comparison of mean velocity and turbulence profile for $R^* = 101 \times 10^5$ ($Re_d \leq 5.7 \times 10^6$).

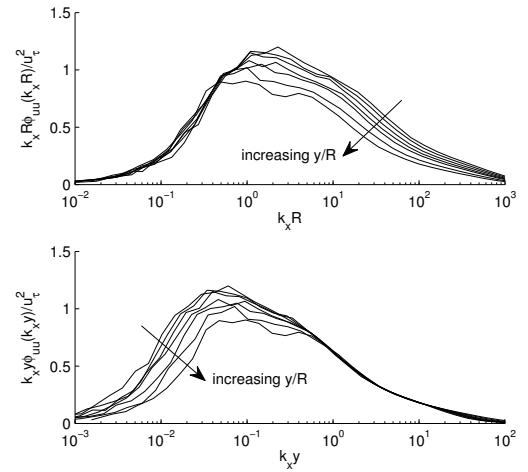


Figure 8. Premultiplied power spectrum at $R^+ = 37000$, scaled using (a) R and (b) y . Points shown are in the logarithmic layer, ranging from $y/R = 0.026$ ($y^+ = 970$) to $y/R = 0.10$ ($y^+ = 3700$)

locity profile are also evident in the turbulence profile. Since the flow experiences roughness effects for $Re_D > 7 \times 10^5$, at the Reynolds number shown in figure 7, the mean velocities are shifted to lower U^+ values relative to the smooth-walled logarithmic profile, but the slope and overall shape of the profile is not altered by the effects of roughness (assuming that Townsend's hypothesis is valid). In figure 7, three different regions have been identified: (1) the near wall region containing the power-law like behavior in the mean velocity profile and in the Reynolds stress profile the boundary of this region corresponds to the location of the outer peak; (2) the logarithmic region in both the mean velocity and Reynolds stress profiles; and (3) a wake region for $y/R > 0.1$ where the mean velocity exhibits outer-scaling and the Reynolds stress decreases to the centerline level.

To examine the spectral behavior, figure 8 shows the streamwise velocity power spectrum at $Re_D = 2 \times 10^6$ ($R^+ = 3.7 \times 10^4$), premultiplied by the streamwise wavenumber $k_x = 2\pi f/U$, where f is frequency and U is the local mean velocity.

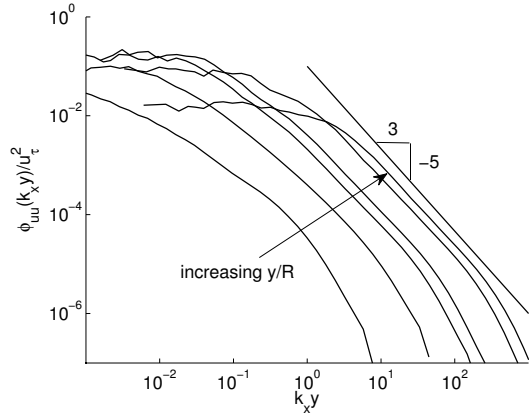


Figure 9. Power spectrum at $R^+ = 37000$ in log-log form. Locations $y/R = [0.001, 0.01, 0.1, 0.5, 1.0]$ shown.

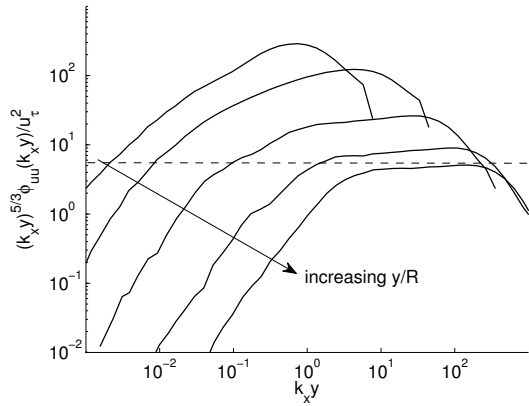


Figure 10. Power spectrum premultiplied by $k_x^{5/3}$ at $R^+ = 37000$. Locations $y/R = [0.001, 0.01, 0.1, 0.5, 1.0]$ shown.

Several locations in the logarithmic layer are shown. We see that within this region the expected low wavenumber R -scaled (figure 8a) and intermediate wavenumber y -scaled (figure 8b) behavior is convincingly demonstrated. What is not evident, however, is the existence of a k_x^{-1} overlap region where both R and y scalings co-exist, as predicted by Perry et al. [1986]. Such a region would appear as a plateau in the spectra, which is not evident.

Figure 9 shows power spectra measured at the same Reynolds number as in figure 8, but in conventional log-log form and with locations selected from across the entire pipe. We see clear evidence of an inertial subrange in the form of a $k_x^{-5/3}$ decay in the spectra, particularly in the outer layer. To examine this region in more detail, we premultiply the spectra by $k_x^{5/3}$, as shown in figure 10. We see that at this Reynolds number the spectra do not show an extended region of $k_x^{-5/3}$, but when the Reynolds number is increased to $R^+ = 1.01 \times 10^6$, as shown in figure 11, we see a true inertial subrange spanning roughly a decade in wavenumber at $y/R = 0.5$ and nearly two decades at $y/R = 1.0$.

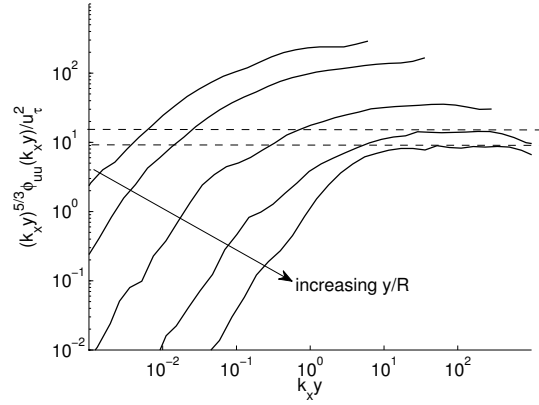


Figure 11. Power spectrum premultiplied by $k_x^{5/3}$ at $R^+ = 101000$. Locations $y/R = [0.001, 0.01, 0.1, 0.5, 1.0]$ shown.

CONCLUSIONS

Experiments were performed in a turbulent pipe flow over a Reynolds number range extending from $Re_D = 4.2 \times 10^4$ to 5.6×10^6 . To obtain highly resolved measurements in space and time of the streamwise component of the velocity, a Nano-Scale Thermal Anemometry Probe was used with a sensing length of only $60 \mu\text{m}$. The results of this study confirms that the inner peak in the turbulent intensity is invariant with Reynolds number, and that an outer peak appears further from the wall at very high Reynolds number. In addition, at extreme Reynolds numbers, the streamwise Reynolds stress exhibits logarithmic scaling behavior, which is shown experimentally here for the first time. The regions of the turbulence scaling correspond very well with identifiable regions in the mean velocity. Finally, power spectra within the logarithmic region confirm the expected inner and outer scaling behavior but a distinct region of k_x^{-1} is not observed. The $k_x^{-5/3}$ variation expected in the inertial subrange is only seen at the very highest Reynolds numbers for $y/R > 0.5$.

ACKNOWLEDGEMENTS

This work was supported by ONR Grant N00014-09-1-0263 (Program Manager Ron Joslin) and NSF Grant CBET-1064257 (Program Manager Henning Winter).

REFERENCES

- M. Hultmark, S. C. C. Bailey, and A. J. Smits. Scaling of near-wall turbulence in pipe flow. *J. Fluid Mech.*, 649:103–113, 2010.
- J. Jiménez. Turbulent flows over rough walls. *Annu. Rev. Fluid Mech.*, 36:173–196, 2004.
- L. I. Langelandsvik, G. J. Kunkel, and A. J. Smits. Flow in a commercial steel pipe. *J. Fluid Mech.*, 595(323-339):323–339, 2007.
- B. J. McKeon, J. Li, W. Jiang, J. F. Morrison, and A. J. Smits. Further observations on the mean velocity distribution in

- fully developed pipe flow. *J. Fluid Mech.*, 501:135–147, 2004.
- J. F. Morrison, B. J. McKeon, W. Jiang, and A. J. Smits. Scaling of the streamwise velocity component in turbulent pipe flow. *J. Fluid Mech.*, 508:99–131, 2004.
- A. E. Perry, S. M. Henbest, and M. S. Chong. A theoretical and experimental study of wall turbulence. *J. Fluid Mech.*, 165:163–199, 1986.
- A. J. Smits, J. Monty, M. Hultmark, S. C. C. Bailey, M. Hutchins, and I. Marusic. Spatial resolution correction for turbulence measurements. *J. Fluid Mech.*, page In press, 2011.
- A. A. Townsend. *The Structure of Turbulent Shear Flow*. CUP, Cambridge, UK, 1976.
- M. Vallikivi, M. Hultmark, S. C. C. Bailey, and A. J. Smits. Nano-scale probes for turbulence measurement. *Science*, page submitted, 2010.
- M. V. Zagarola and A. J. Smits. Mean-flow scaling of turbulent pipe flow. *J. Fluid Mech.*, 373:33–79, 1998.